STUDY OF BEAM TRANSPORT LINES FOR A BIOMEDICAL RESEARCH FACILITY AT CERN BASED ON LEIR *

D. Abler[†], University of Oxford, Oxford, UK
C. Carli, A. Garonna, CERN, Geneva, Switzerland
K. Peach, John Adams Institute, Oxford, UK

Abstract

The Low Energy Ion Ring (LEIR) at CERN has been proposed to provide ion beams with magnetic rigidities up to 6.7 T.m for biomedical research, in parallel to its continued operation for LHC and SPS fixed target physics experiments. In the context of this project, two beamlines are proposed for transporting the extracted beam to future experimental end-stations: a vertical beamline for specific low-energy radiobiological research, and a horizontal beamline for radiobiology and medical physics experimentation. This study presents a first linear-optics design for the delivery of 1–5 mm FWHM pencil beams and 5 cm × 5 cm homogeneous broad beams to both endstations. High field uniformity is achieved by selection of the central part of a strongly defocused Gaussian beam, resulting in low beam utilisation.

ION-BEAM FACILITY AT CERN

The establishment of a biomedical ion-beam research facility at CERN, based on the existing Low Energy Ion Ring (LEIR), has been proposed [1] to provide beam time for pre-clinical studies. In addition to upgrades of the LEIR injector [2] and a new slow extraction from LEIR [3, 4], new beam transfer lines are needed to guide the extracted beam towards the adjacent 'South Hall' where experimental endstations and related infrastructure can be installed.

Designs for a horizontal and a vertical beamline, connected to a common extraction and transfer line, were studied to provide suitable beams for the two main use-cases of this new facility: medical physics and instrumentation experiments, as well as *in-vitro* cell survival experiments.

DESIGN CONSTRAINTS AND METHODOLOGY

Beam Requirements for Biomedical Experiments

Beam requirements and design criteria are summarised in Table 1: *In-vitro* cell survival experiments demand a sufficiently wide range of beam energies to allow measurements at different points along the Bragg curve, from its rising slope to the Bragg peak. Vertical beam delivery is considered advantageous to minimise stress on the biological samples and to facilitate experimentation. Beam energies for medical physics experiments need to cover typical treatment depths of 3.5–27.5 cm in tissue. Adjustable beam sizes

Table 1: Beam Requirements. Energies Quoted for $^{12}_{6}C^{6+}$

	Medical Physics	Radiobiology
Ions	mainly p, $^{12}_{6}C$	p to $^{20}_{10}Ne$
Energies	120–400 MeV/u	10–75 MeV/u
Field size	5–10 mm FWHM to 5 cm × 5 cm	
Field uniformity	>90 % across irradiation field	

Table 2: Start Parameters and Matching Constraints

ϵ_{rms} [π mm mrad]	β [m]	D [m]	D'	α
Start parameters at first electrostatic extraction septum:				
Vertical 0.6–4.2	15	0	0	-2.8
Horizontal 2	15	-4	-1	0
Target parameters at end of beam lines:				
Pencil beam 4.5	1	0	0	0
Broad beam 4.5	1500	0	0	–

between 'pencil beam' to 'broad beam' are considered sufficient for both types of studies. Field uniformity constraints are derived from total absorbed dose accuracy of at least ±5 % and preferably better than ±2 %.

Characteristics of Slow-Extracted Beam

In horizontal phase space, the slow extracted beam is characterised by very small divergence and a width of several mm, defined by the maximum spiral step and therefore independent from beam energy. Particle coordinates delimiting this 'bar of charge' were obtained in a preliminary single-particle tracking study for quadrupole-driven slow-extraction from LEIR [5] which has been refined recently [3,4]. Estimates for horizontal Twiss parameters were computed following the 'unfilled ellipse' approach [6], modified to allow parameter estimation from a small number of delimiting particles [5], and $\alpha_x = 0$ was assumed at the electrostatic extraction septum (ES). Vertical phase space properties of the slow-extracted beam are similar to those of the circulating beam at the ES. Table 2 summarises the beam parameters used in this study.

Beam Delivery

Due to the slow extraction process, the shape of the horizontal beam profile depends on the phase advance between first extraction septum and target [7]. Multiple scattering on a thin foil can be used [8,9] to transform the extracted 'bar of charge' into an approximately Gaussian distribution. Applying the formula for the effect of a thin scatterer on the Twiss parameters and beam emittance [10], approximately equal

emittances in both transverse planes can be obtained by adjusting the thickness of the scatter foil and β functions at its position. This study assumes that $\epsilon_{rms, x/y} = 4.5\pi$ mm mrad after scattering is achievable for all energies, using scatter foils with up to several 10^{-3} radiation lengths thickness.

Based on the assumption of Gaussian beams after scattering, the study exploits the relative uniformity of their central region for producing homogeneous broad beams. By strongly defocusing the beam in both planes, the rms beam half width $\sigma = \sqrt{\beta \, \epsilon_{rms}}$ on the target can be increased until the desired level of dose uniformity I/I_0 across a given sample area is reached. The portion of the beam exceeding sample dimensions has to be collimated. Figure 1 indicates that $\sigma = 77$ mm (left scale) would be sufficient to irradiate a 5 cm $\times$ 5 cm target area with intensity variations of $\pm 5\%$ ($I/I_0 = 0.9$), using 6.5 % of the beam particles (right scale).

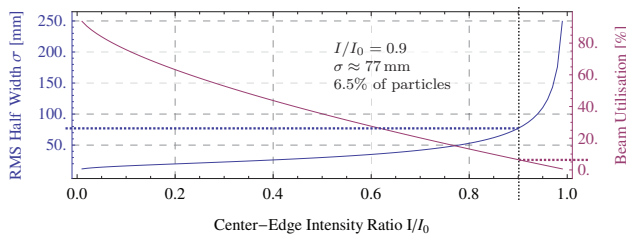Figure 1: Required rms beam half width σ (left scale) and beam utilisation (right scale) in function of maximum intensity variation I/I_0 across 5 cm $\times$ 5 cm irradiation field.

Space Constraints

While the 'South Hall' provides ample surface area for installation of beamlines and other infrastructure, vertical space availability is limited due to transport cranes installed across the site. This study assumes the vertical beamline to be directed 'upwards' so that biological samples are irradiated 'from below'. Placement of the vertical beamline is therefore constrained to an area of maximum vertical space availability, delimited by dashed red lines in Fig. 2, ~7.5 m from ground level compared to ~5.5 m at any other location. With an installation height of ~1.5 m for LEIR, the vertical beam line, including experimental endstation, is thus limited to a maximum height of ~6 m.
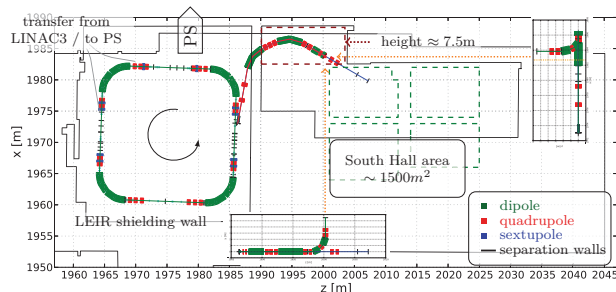

Figure 2: LEIR and proposed beamlines in 'South Hall'.

RESULTS

A fully stripped carbon ion beam $^{12}_{6}C^{6+}$ with $q/A = 1/2$ was assumed for this study since very similar charge-over-mass ratio can be achieved for most elements of biomedical interest, Table 1. *MADX* [11] was used for beam optics and beamline matching. Beam envelopes were computed using the $2.5 \, \sigma$ beam half width based on the rms emittances given in Table 2 and assuming maximum momentum spread $\Delta p/p = \pm 0.2$‰ throughout the line. Matching constraints in the target planes of both beamlines are listed in Table 2. Figure 2 shows LEIR with the proposed beam transport lines: An extraction line from LEIR with horizontal bend towards the adjacent 'South Hall', extensions for a horizontal (up to 430 MeV/u) and for a vertical beamline (up to 75 MeV/u).

Beam Transport Lines and Optical Functions

The *common transport line* (Fig. 3a upstream of *qc4*) is designed to remove the initial negative horizontal dispersion using a quadrupole triplet (*qcb1, qcb2, qcb3*), and to provide a suitable position ($\beta_x \gg \beta_y$, $\Delta\mu_x$ from ES multiple of π) for the placement of a thin scatter foil (between *qc3* and *qc4*). The extracted beam is assumed to enter LEIR element *KFH3234* at $x = -42$ cm, $x' = -140$ mrad so that a first quadrupole *qc1* can be placed 3.5 m downstream of the entry to *KFH3234*. The horizontal bending structure (118°, $B\rho = 6.7$ T.m) is modelled by identical *SBEND* segments with half-gap of 40 mm. Its bending angle and length are chosen to permit installation of the vertical beamline at the location of maximum vertical space availability while respecting existing building walls. The *vertical beamline* extension (Fig. 3a downstream of *qc4*) starts with an achromatic bend (90°, $B\rho = 2.6$ T.m) that is modelled by two 45° *SBEND* segments with half-gap of 40 mm and a defocusing quadrupole *qvb1* centred between them. A further quadrupole doublet (*qv1, qv2*) allows (de-)focusing of the beam onto the target plane, assumed at a height of 5.5 m relative to the accelerator structures. The *horizontal beamline* (Fig. 3b) extends the common transport line by a further quadrupole doublet (*qh1, qh2*), installed downstream of the vertical bend.

Both beamlines allow the β functions in the target plane to be adjusted over a range of β =1–1500 m, as illustrated in Figs. 3a and 3b, and thus fulfil field size and homogeneity criteria outlined in Table 1. Enforcement of achromatic beam transfer through the common horizontal bending segment defines the coefficients of quadrupoles up to *qcb3*, so that beam functions in this segment show little dependency on target parameters. Horizontal (vertical) β functions at the scatter foil can be adjusted between 40–80 m (5–10 m) approximately.

Characteristics of Optical Elements

Lengths for all 12 quadrupoles in this study were assumed equal to LEIR quadrupoles ($l = 0.52$ m). Table 3 reports maximum gradients and largest beam envelopes.

(a) Common beam transport line and vertical extension.
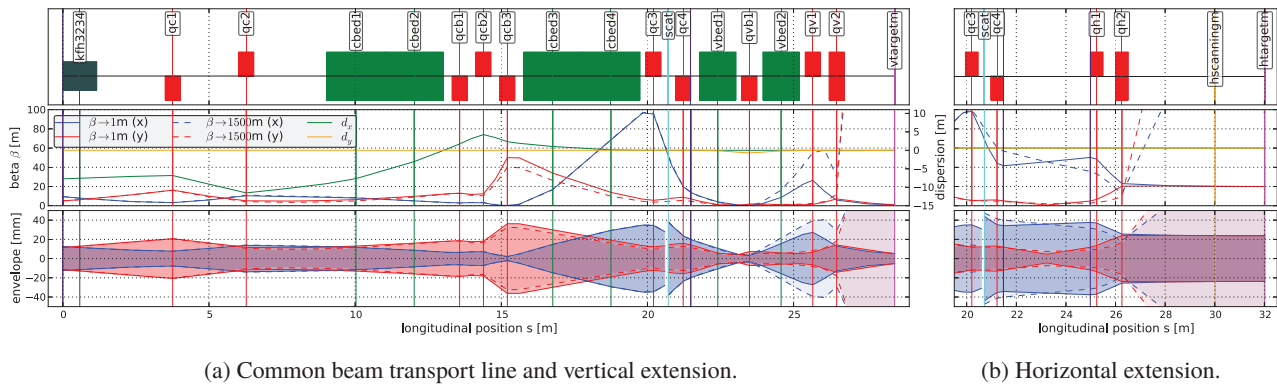
(b) Horizontal extension.

Figure 3: Elements, Twiss functions and beam envelopes for (a) common transport line and vertical beam line extension, (b) and horizontal beamline extension; for $\beta = 1$ m (solid lines) and $\beta = 1500$ m (dashed lines) in target plane.

Table 3: Maximum quadrupole gradients k [T m^{-1}] and beam envelopes BE [mm].

(a) Common beam transport line (430 MeV/u).

	qc1	qc2	qcb1	qcb2	qcb3	qc3	qc4
k	-4.5	3.4	-5.3	21.8	-11.9	9.5	-11.4
BE	±21	±14	±19	±18	±36	±35	±42

(b) Vertical and horizontal extensions (75 and 430 MeV/u).

	qvb1	qv1	qv2	qh1	qh2
k [T m^{-1}]	-10.4	6.5	22.4	8.3	20.9
BE [mm]	±7	±40	±31	±37	±25

DISCUSSION

The chosen broad-beam delivery mechanism requires very strong beam defocusing and collimation. Therefore, further study of its implications for radiation protection and beam stability is needed to conclude on its suitability.

The following upgrades to the proposed beamlines may be envisaged: A pencil-beam scanning system may be added to the horizontal beamline by inserting horizontal and vertical scanning magnets downstream of *qh2*. This setup would resemble beam delivery in modern clinical centres and also be capable of providing homogeneous broad beams through re-scanning. Installation of such a system in the vertical beamline is challenging, however, scanning-like functionality (for thin and low-weight samples) could be achieved through a motorised setup table. Two upgrade options should be studied to improve broad beam delivery in the vertical beamline: Installation of a beam 'wobbling' mechanism in the remaining ~1.8 m drift between *qv2* and target plane, and the use of non-linear optical elements for flattening the Gaussian beam profile in both transverse planes. Latter requires the installation of two octupoles at locations where horizontal or vertical beam size dominate, respectively. In order to ensure Gaussian beam profiles at their location, the thin scatter foil has to be moved towards the beginning of the common beam transport line, or the spacing between horizontal and vertical bend needs to be enlarged to provide

space for additional optical elements. This is not possible under the positioning constraints assumed here.

Space could be gained by installing the vertical beamline underground (irradiation 'from above'). Possible locations, restricted by trenches and cable ducts across the site, are delimited by dashed green lines in Fig. 2. While underground installation necessitates the creation of access, it may be less critical for radiation protection aspects.

CONCLUSION

An optical design for beam transfer lines from LEIR to future experimental endstations in the adjacent 'South Hall' has been developed. It consists of a common transport line and two separate beamline extensions for horizontal and vertical beam delivery. Both lines allow for adjusting beam sizes from 5 mm FWHM pencil beams up to very large beams. Inhomogeneities in the central 5 cm × 5 cm of their Gaussian profile remain below ±5 %.

ACKNOWLEDGEMENT

REFERENCES

[1] M. Dosanjh et al., Br J Radiol 2013; 86:20120660.

[2] J. Stafford-Haworth et al., Rev Sci Instrum 2014; 85:02A923.

[3] A. Garonna et al., CERN-ACC-2014-0061, 2014.

[4] A. Garonna et al., IPAC'14, MOPRI094, These proceedings.

[5] D. Abler, PhD thesis, University of Oxford, To be published.

[6] M. Benedikt et al., NIMPA 1999; 430:523-533.

[7] L. Badano et al., "PIMMS I", CERN-PS-99-010-DI, 1999.

[8] T. Furukawa et al., EPAC 2006 Proceedings, p. 2322-2324.

[9] N. Tsoupas et al., PRSTAB 2007; 10:024701.

[10] A.T. Maier, CERN-PS-98-061-DI, 1998.

[11] MAD-X home page, http://mad.web.cern.ch/mad